9. Segovia, N., Pena, P. and Tamex, E., Radon survey in Mexico City. *Nucl. Tracks Radiat. Meas*., 1991, **19**, 405–408.
10. Pena, P., Segovia, N., Azorin, J. and Mena, M., Soil radon and gamma-dose rate at a coastal region in Mexico. *J. Radioanal. Nucl. Chem*., 2001, **247**, 39–43.
11. Choubey, V. M., Ramola, R. C. and Sharma, K. K., Soil gas and indoor radon studies in Doon Valley, India. *Nucl. Geophys*., 1994, **8**, 49–54.
12. Ruckerbaur, F. and Winkler, R., Radon concentration in soil gas: A comparison of methods. *Appl. Radiat. Isot*., 2001, **55**, 273–280.
13. Ramachandran, T. V., Lalit, B. Y. and Mishra, U. C., Measurement of radon permanently through some membranes. *Nucl. Tracks Radiat. Meas*., 1987, **13**, 81–84.
14. Mayya, Y. S., Eappen, K. P. and Nambi, K. S. V., Methodology for mixed field inhalation in monazite areas using a twin-cup dosimeter with three-track detector. *Radiat. Prot. Dosim*., 1998, **77**, 177–184.
15. Eappen, K. P. and Mayya, Y. S., Calibration factors for LR-115 (type-II) based radon–thoron discriminating dosimeter. *Radiat. Meas*., 2004, **38**, 5–17.
16. Srivastava, G. K., Raghavayya, M., Khan, A. H. and Kotrappa, P., A low level radon detection system. *Health Phys*., 1984, **46**, 225–228.
17. Sannappa, J., Paramesh, L. and Venkataramaiah, P., Study of radon exhalation rate in soil and air concentrations. *Indian J. Phys. B*, 1999, **73**, 629–639.
18. *EML Procedure Manual*, *26th Edition* (eds Volchok, H. L. and dc Planque, G.), Environmental Measurement Laboratory, New York, 1983.
19. IAEA/RCA, Regional Workshop on Environmental Sampling and Measurement of Radioactivity for Monitoring Purposes, BARC, Kalpakkam, 1989, pp. 85–95.
20. UNSCEAR, Ionizing radiation sources and biological effects. Report to the UN General Assembly, New York, 1982.
21. Schery, S. D., Gaedert, D. H. and Wilkening, M. H., Factors affecting exhalation of radon from a gravely sandy loam. *J. Geophys. Res*., 1984, **89**, 7299–7309.
22. Thomas, D. M., Cotter, J. M. and Holford, D., Experimental design for soil gas radon monitoring. *J. Radioanal. Nucl. Chem*., 1992, **161**, 313–323.
23. Vohra, K. G., Subbaramu, M. C. and Mohan Rao, A. M., Measurement of radon in soil gas. *Nature*, 1964, **4914**, 37–39.
24. Vaupotic, J., Andjelov, J. and Kobal, I., Relationship between radon concentrations in indoor air and in soil gas. *Environ. Geol.*, 2002, **42**, 583–587.
25. Shweikani, R. and Hushari, M., The correlations between radon in soil gas and its exhalation and concentration in air in the southern part of Syria. *Radiat. Meas.*, 2005, **40**, 699–703.

ACKNOWLEDGEMENTS. We thank Dr Mayya and his group at BARC, Mumbai for providing dosimeter cups designed by them and other equipment under the coordinated BRNS project. We also thank Dr M. Raghavayya, BARC, Mysore for useful discussions and constant encouragement throughout the work.

Received 6 December 2006; revised accepted 24 March 2008

Identifying biomass burned patches of agriculture residue using satellite remote sensing data

Milap Punia[1], Vinod Prasad Nautiyal[2] and Yogesh Kant[2,*]

[1]Centre for the Study of Regional Development, School of Social Sciences, Jawaharlal Nehru University, New Delhi 110 067, India
[2]Indian Institute of Remote Sensing, 4 Kalidas Road, Dehradun 248 001, India

The combine harvesting technology which has become common in the rice–wheat system in India leaves behind large quantities of straw in the field for open residue burning, and Punjab is one such region where this is regularly happening. This becomes a source for the emission of trace gases, resulting in perturbations to regional atmospheric chemistry. The study attempts to estimate district-wise burned area from agriculture residue burning. The feasibility of using low resolution (MODIS) and moderate resolution (AWiFS) satellite data for estimation of burned areas is shown. It utilizes thermal channels of MODIS and knowledge-based approach for AWiFS data for burned area estimation. A hybrid contextual test-fire detection and tentative-fire detection algorithm for satellite thermal images has been followed to identify the fire pixels over the region. The algorithm essentially treats fire pixels as anomalies in images and can be considered a special case of the more general clutter or background suppression problem. It utilizes the local background around a potential fire pixel, and discriminates fire pixels and avoids the false alarm. It incorporates the statistical properties of individual bands and requires the manual setting of multiple thresholds. Also, a decision-tree classification based on See5 algorithm is applied to AWiFS data. When combined with image classification using a machine learning decision tree (See5) classification, it gives high accuracy. The study compares the estimated burned area over the region using the two algorithms.

Keywords: Burned patches, decision-tree classifier, knowledge-based classification, thermal band.

BIOMASS burning is a major source of many atmospheric particulates and trace gases, which have a major impact on climate; it also affects human health causing respiratory problems. It is recognized as a significant global source of emissions, contributing as much as 40% of gross carbon dioxide and 38% of tropospheric ozone[1]. It has significant impact on the atmospheric chemistry and biogeochemical cycles[2], radiative energy balance and climate[3,4]. Smoke particles from biomass burning have direct radiative impact by scattering and absorbing shortwave

*For correspondence. (e-mail: yogesh@iirs.gov.in)

radiation and indirect radiative impact by serving as cloud-condensation nuclei and changing the cloud micro-physical and optical properties[5]. Studies suggest that biomass burning has increased on a global scale over the last 100 years and computer calculations indicate that a hotter earth resulting from global warming will lead to more frequent and larger fires[6].

Combine harvesting technologies, which have become common in the rice–wheat system (RWS) in India, leave behind large quantities of straw in the field for open burning of residues. Punjab has about 2,647,000 ha under paddy cultivation that yields roughly 100 million tonnes of rice straw and about three-fourth of crop residue amounting to 70–80 million tonnes of rice is disposed-off by burning[7]. The easy option left for proper management of left-over straw for farmers is to burn it in the field as the decomposition of residues takes a long time. Such burning results in perturbations to the regional atmospheric chemistry due to emissions of trace species like CO_2, CO, CH_4, N_2O, NO_x, NMHCs, aerosols and is also a health hazard to local inhabitants. The emission of CH_4, CO, N_2O and NO_x has been estimated to be about 110, 2306, 2 and 84 Gg respectively, in 2000 from rice and wheat straw burning in India[8]. Residue burning also causes nutrient and resource loss, and reduces total N and C in the topsoil layer, thus calling for improvement in harvesting technologies and sustainable management of the RWS[9].

In studies related to biomass burning, satellite data owing to wide swath, good temporal and spectral resolution, find importance in detecting and monitoring of fire in a quantitative and qualitative manner. There are two main monitoring strategies which are analysed – detection of burned areas at fine, moderate spatial resolution and detection of active fires at coarse spatial resolution at high temporal frequency. This study attempts at the use of high temporal satellite (coarse spatial resolution) Moderate Resolution Imaging Spectroradiometer (MODIS) and moderate resolution (low temporal resolution) Advanced Wide Field sensor (AWiFS) data in estimating burned areas. The thermal channels of day and night-time MODIS data and knowledge-based approach for AWiFS data have been utilized for deriving burned areas.

Punjab, with a geographical area of 50,362 sq. km, forms a part of the Indus plain. It lies between 29°33′–32°31′N lat. and 73°53′–76°55′E long., bounded by Pakistan to its west, Jammu and Kashmir to its north, Himachal Pradesh to its east and northeast, Haryana to its east and southeast, and Rajasthan to its west. Most of Punjab is a gently undulating plain. The Shiwalik hills rise in the northeast. To its south extend narrow foothills that end in the plains further below (Figure 1).

Punjab is one of the smallest states in India, representing 1.6% of its geographical area and 2.6% of its cropped area. Agriculture occupies the most prominent place in the State's economy. Known as the granary of India, Punjab has made enormous contributions to the national pool of foodgrains, i.e. around 70% of wheat and 50% of rice. As against an all-India average of 51%, Punjab has 85% of its area under cultivation. The state, on an average, accounts for 23% of wheat, 14% of cotton and 10% of rice production of the whole country. It is only in the districts of Ropar and Hoshiarpur that the cultivated area is less than 60% of the total. It is in these districts that considerable land is covered by the Shiwalik hills and the beds of seasonal streams that cannot be brought under cultivation. However this growth of agriculture is associated with high input in terms of fertilizers, pesticides, water, etc.

The State has witnessed a paradigm shift in its cropping pattern. From multi-cropped practice, it has shifted to a mono-cropped one. Area under high-input intensive crops like wheat, paddy and cotton is increasing at the cost of traditional low-inputs crops. Important soil-enriching crops like gram and pigeonpea have declined significantly, and area under maize, millet and groundnuts has

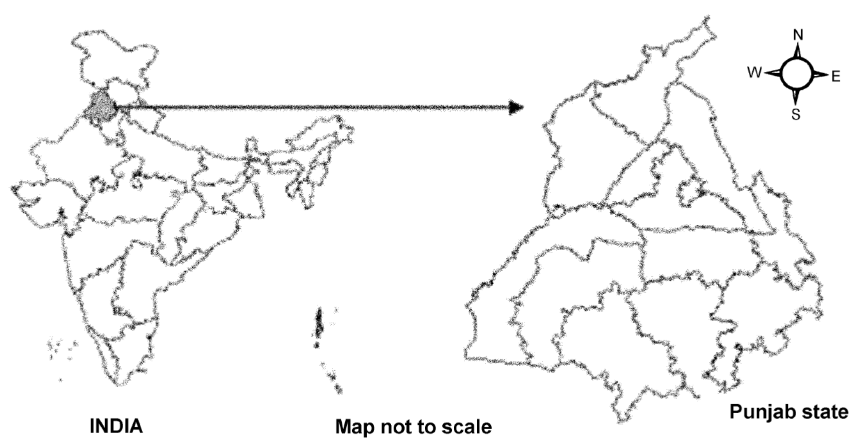

Figure 1. Location of the study area.

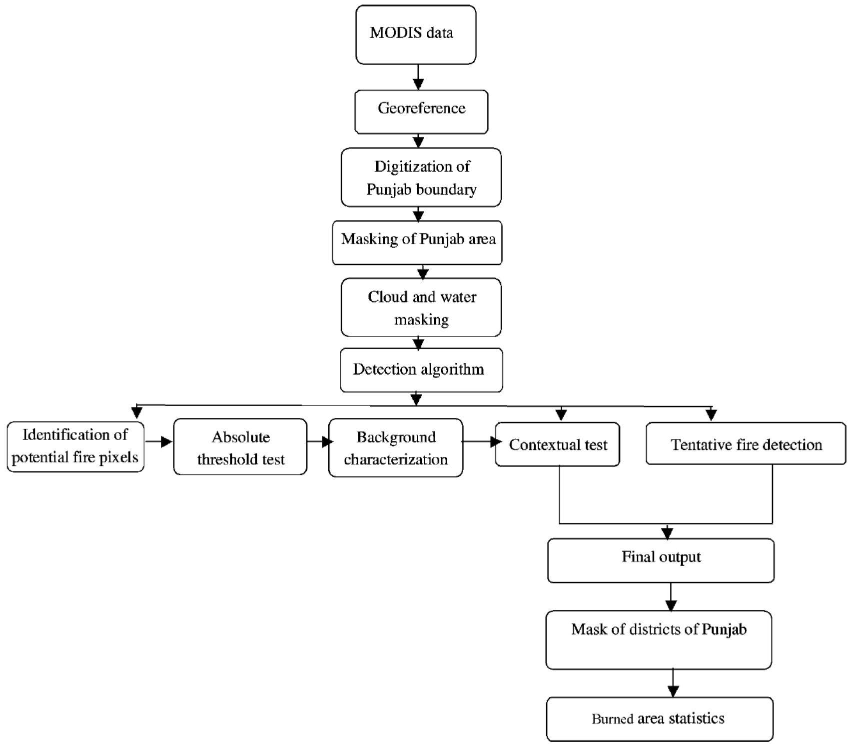

Figure 2. Flow chart for extracting potential burned pixels using MODIS data.

given way to rice during Kharif season and that from gram, repressed/mustard and barley has given way to wheat during Rabi season. At present, about 95% of the total foodgrain production in Punjab is from rice and wheat[9].

The study attempts to utilize moderate spatial resolution AWiFS and low resolution MODIS data in estimating the burned pixels. Data of AWiFS having spatial resolution of 56 m on-board *IRS-P6* of 15 May 2005 and day and night-time MODIS data on-board *Terra* of 15 May 2005 have been used. AWiFS data are used for extracting burned areas using knowledge-based classification approach, whereas thermal bands of MODIS data are used for extracting the potential burned pixels over the study area.

The fire-detection algorithm[10] uses brightness temperature derived from MODIS 4 μm and 11 μm channels (denoted by T_4 and T_{11} respectively). The MODIS instrument has two channels (in the 4 μm wavelength) number 21 (saturation at nearly 500 K) and number 22 (saturation at nearly 331 K), both of which are used in the detection algorithm. Since the low saturation channel 22 is less noisy and has a smaller quantization error, T_4 is derived from this channel, whenever possible. However, when channel 22 saturates and has missing data, it is replaced with the high-saturation channel to derive T_4. T_{11} is computed from the 11 μm channel (channel 31), which saturates at approximately 400 K for the terra MODIS and 340 K for aqua MODIS[10]. The 12 μm channel (no. 32) is used for cloud masking brightness temperature and is denoted by T_{12}. The 250 m resolution red and near-infrared channels aggregate to 1 km are used to reject false alarm and mask cloud. These reflectances are denoted by $\rho_{0.65}$ and $\rho_{0.86}$ respectively. Figure 2 shows the algorithm for extracting burned patches using MODIS data.

The purpose of the detection algorithm is to identify fire pixels. The algorithm examines each pixel of the MODIS swath and ultimately assigns it to one of the following classes: missing data, cloud, water, non-fire, fire, or unknown. Pixels lacking valid data are immediately classified as missing data and excluded from further consideration.

Under identification of potential fire pixels, a preliminary classification is used to eliminate obvious non-fire pixels. The pixels that remain are considered in subsequent tests to determine if they do in fact contain an active fire. A daytime pixel is identified as a potential fire pixel if $T_4 > 310$ K, $\Delta T > 10$ K and $\rho_{0.86} < 0.3$, where $\Delta T = T_4 - T_{11}$. For night-time pixels, the reflective test is omitted and the T_4 thresholds reduce to 305 K. Pixels failing these preliminary tests are immediately classified as non-fire pixels. There are two logical paths through which fire pixels can be identified. The first consists of a simple absolute threshold test. This threshold must be set sufficiently high so that it is triggered only by unambiguous fire pixels, i.e. those with little chance of being a false alarm.

The absolute threshold criterion remains identical to the one employed in the original algorithm[11]:

$$T_4 > 360\text{ K (320 K at night)}. \qquad (1)$$

In the next phase of the algorithm[10], which is performed regardless of the outcome of the absolute threshold test, an attempt is made to use the neighbouring pixels to estimate the radiometric signal of the potential fire pixel in the absence of fire. Valid neighbouring pixels in a window centred on the potential fire pixel are identified and used to estimate a background value. Within this window, valid pixels are defined as those that (a) contain usable observations, (b) are located on land, (c) are not cloud-contaminated, and (d) are not background fire pixels. Background fire pixels are in turn defined as those having $T_4 > 325$ K and $\Delta T > 20$ K for daytime observations, or $T_4 > 310$ K and $\Delta T > 10$ K for nighttime observations.

If the background characterization is successful, a series of contextual threshold tests are used to perform relative fire detection. These look for the characteristic signature of an active fire in which both the 4 μm brightness temperature (T_4) and the 4 and 11 μm brightness temperature difference (ΔT) depart substantially from that of the non-fire background. Relative thresholds are adjusted based on the natural variability of the background. The tests are:

$$\Delta T > \Delta\overline{T} + 3.5\delta_{\Delta T}, \qquad (2)$$

$$\Delta T > \Delta T + 6K, \qquad (3)$$

$$T_4 > \overline{T}_4 + 3\delta_4, \qquad (4)$$

$$T_{11} > \overline{T}_{11} + \delta_{11} - 4k. \qquad (5)$$

Among these conditions, the first three isolate fire pixels from the non-fire background. The factor 3.5 appearing in test (2) is larger than the corresponding factor of 3 in test (4) to help adjust for partial correlation between the 4 and 11 μm observations. Condition (5) which is restricted to daytime pixels, is primarily used to reject small connective-cloud pixels that can appear warm at 4 μm (due to reflected sunlight) and cool in the 11 μm thermal channel. It can also help to reduce coastal fire alarms that sometimes occur when cooler-water pixels are unknowingly included in the background window. Any test based on δ_{11}, however, risks rejecting very large fires since these will increase the 11 μm background variability substantially. In this position one can tentatively identify pixels containing active fires. For night-time fires, this will in fact be an unambiguous, final identification. For daytime pixels, three additional steps are used to help eliminate false alarms caused by sun glint, hot desert surfaces, and coasts or shorelines.

A daytime pixel is tentatively classified as a fire pixel if:

{test (1) is true} or,
{test (2) – test (4)} are true and {test (5) is true}.

Otherwise it is classified as fire pixels.

A night-time candidate fire pixel is definitely classified as a fire pixel if:

{test (1) is true} or, {test (2) – test (4) is true}.

Otherwise it is classified as non-fire.

For daytime and night-time pixels for which the background characterization had failed, i.e. an insufficient number of valid neighbouring pixels were identified, only test (1) is applied in this step. If not satisfied, the pixel is classified as unknown, indicating that the algorithm was not able to unambiguously render a decision.

Figure 3 shows a flowchart for extracting burned patches using AWiFS data. To extract burned areas, the See5 algorithm[12], which is basically a decision-tree classifier, has been used. The advantage of the decision-tree classifier over traditional statistical classifiers is its simplicity, ability to handle missing and noisy data, and non-parametric nature.

Let us now consider the decision tree algorithm.

Step 1: Let T be the set of training instances.
Step 2: Choose an attribute that best differentiates the instances in T.
Step 3: Create a tree node whose value is the chosen attribute.

- Create child links from this node, where each link represents a unique value for the chosen attribute.
- Use the child link values to further subdivide the instances into subclasses.

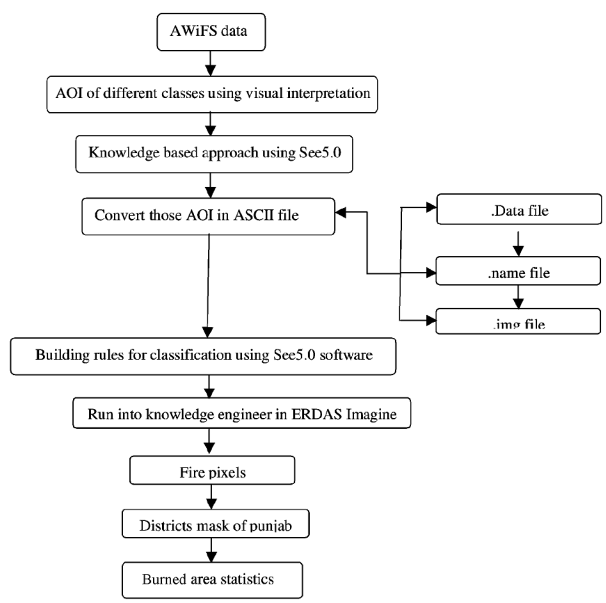

Figure 3. Flow chart for extracting burnt pixels using AWiFS data. AOI, area of interest; ASCII, American Standard Code for Information Interchange; ERDAS, Earth Resources Data Analysis System.

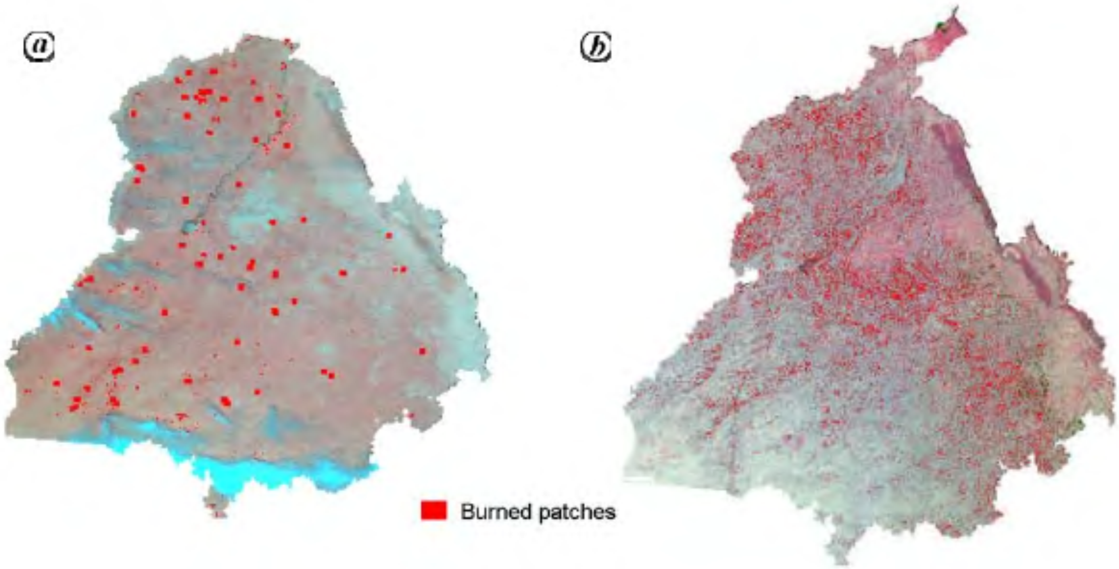

Figure 4. Fire patches extracted from (***a***) MODIS and (***b***) AWiFS data of 15 May 2005.

Step 4: For each subclass created in step 3:

- If the instances in the subclass satisfy predefined criteria or if the set of remaining attribute choices for this path is null, specify the classification for new instances following this decision path.
- If the subclass does not satisfy the criteria and there is at least one attribute to further subdivide the path of the tree, let *T* be the current set of subclass instances and return to step 2.

It is obvious that if the rules are not complete after tracing through the decision tree, some pixels will remain unclassified. Therefore, the efficiency and performance of this approach is strongly affected by tree structure and choice of features selected for training.

Once the classification rules are generated using the decision-tree classifier, they can serve as a knowledge base. This knowledge base can be used for classification of the satellite images. Three approaches were followed to use the extracted rules for the classification. In first approach, classification rules were used directly with the knowledge-based classifier to classify the image. In the second approach prior probability of the class distribution was used to classify the image. A new method was proposed to calculate the prior probability from the already classified image using the first approach. The third approach uses the post-classification sorting method to reclassify pixels which were misclassified during maximum likelihood classification. The AWiFS image was classified with extracted classification rules using the knowledge-based classifier in ERDAS. The extracted classification rules served as the knowledge base to classify the image.

In the present study an improved, contextual, active fire-detection algorithm for the MODIS data has been applied. The probability of detection is strongly dependent upon the temperature and area of the fire being observed. Figure 4 *a* shows the burned area derived using the day and night MODIS datasets. The ideal condition is when the fire is observed at a fairly homogeneous surface, the background window contains no fire and the scene is free of clouds and heavy smoke. High thresholds have been used to identify potential fire pixels. Fire shows little or no contrast against the hot, bright surface that can saturate the mid-infrared channel even in the absence of a fire. The high saturation of the MODIS band 21, however, allows detection to proceed largely unhampered.

Figure 5 shows the estimated district-wise potential burned areas over Punjab on 15 May 2005, obtained from MODIS data and the total burned area is found to be around 954.71 sq. km. From the results it can be seen that Gurdaspur, Amritsar, Faridkot and Firozpur districts are severely affected by agriculture residue burning. Bhatinda, Ludhiana, Sangrur, Kapurthala and Hoshiarpur are moderately affected, and Rupnagar, Patiala and Jhalandhar are least affected.

Figure 4 *b* shows the estimated burned areas using AWiFS data obtained from knowledge-based classification approach using See5 algorithm. Figure 6 shows the district-wise burned area distribution and the estimated total burned area is found to be around 4315.35 sq. km. Among these, Amritsar has more burned area (673.99 sq. km) followed by Jhalandhar, Ludhiana, Firozpur and Patiala districts and Rupnagar was the least affected (41.36 sq. km). The difference in the district-wise estimates of burned areas is due to the use of different spatial-resolution sen-

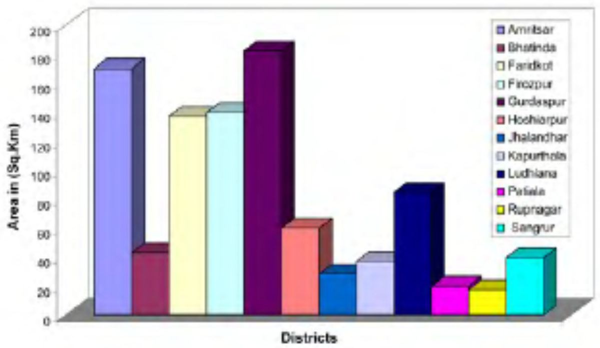

Figure 5. District-wise burned areas over the region using MODIS data of 15 May 2005.

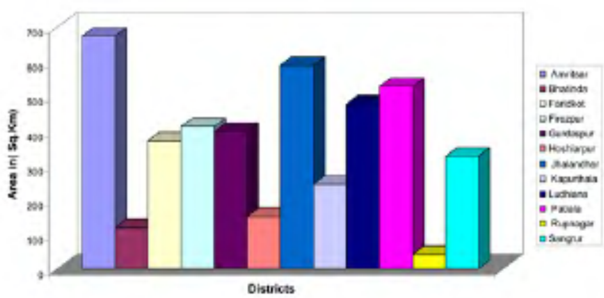

Figure 6. District-wise burned areas over the region using AWiFS data of 15 May 2005.

sors. The hybrid contextual fire detection algorithm helps in the use of thermal bands in monitoring and detection of burnt areas on a regular interval (high temporal frequency) and optical bands from low temporal satellite data to estimate the burned area. The estimates obtained using AWiFS data are the cumulative burned areas generated using the knowledge-based classification, whereas using MODIS dataset the estimates show potential fire pixels.

Mapping of burned biomass is a difficult task, but remote-sensing tools are prove to be promising. The study demonstrates the use and importance of the knowledge-based classification approach using VNIR channels and contextual fire-detection algorithm using thermal channels for identifying and deriving burned areas. It shows the feasibility of using high and low temporal satellite datasets in estimating burned areas. Due to the absence of any field data or other statistics, the satellite-derived district-wise burned areas could not be validated. The difference in the burned area maybe due to the fact that from AWiFS dataset commutative burned area statistics is generated using knowledge-based classification up to 135th Julian day, whereas in the case of MODIS burned area statistics shows potential fire pixels of 135th Julian day. Open field burning of crop residue leads to emission of trace gases like CH_4, CO, N_2O, NO_x, other hydrocarbons and also emission of large amount of particulates composed of a wide variety of organic and inorganic species. From such studies, the spatial extent of burned areas estimated from satellite data would help estimate the amount of trace-gas emissions.

1. Levine, J. S. *et al.*, In *Global Biomass Burning: Atmospheric, Climatic, and Biospheric Implications* (eds Levine, J. S.), The MIT Press, Cambridge, MA, 1991.
2. Crutzen, P. J. and Andreae, M. O., Biomass burning in the tropics: Impact of atmospheric chemistry and biogeochemical cycles. *Science*, 1990, **250**, 1669–1678.
3. Penner, J. E., Dickinson, R. E. and O'Neill, C. A., Effects of aerosols from biomass burning on the global radiation budget. *Science*, 1992, **256**, 1432–1433.
4. Andreae, M. O., Its history, use and distribution and its impact on environment quality and global climate. In *Global Biomass Burning: Atmospheric, Climatic and Biospheric Implications* (ed. Levine, J. S.), MIT Press, Cambridge, MA, 1991, pp. 1–21.
5. Kaufman, Y. J. and Fraser, R. S., The effect of smoke particles on clouds and climate forcing. *Science*, 1997, **277**, 1636–1639.
6. NASA Earth Observatory, http://earthobservatory.nasa.gov/Library/BiomassBurning/
7. Badarinath, K. V. S. and Chand Kiran, T. R., Agriculture crop residue burning in the Indo-Gangetic Plains – A study using IRS-P6 WiFS satellite data. *Curr. Sci.*, 2006, **91**, 1085–1089.
8. Gupta, P. K. *et al.*, Residue burning in rice–wheat cropping system: Causes and implications. *Curr. Sci.*, 2004, **87**, 1713–1715.
9. Gupta, R. K., Naresh, R. K., Hobbs, P. R., Jiaguo, Z. and Ladha, J. K., Sustainability of post-green revolution agriculture: The rice–wheat cropping systems of the Indo-Gangetic Plains and China. In *Improving the Productivity and Sustainability of Rice–Wheat System: Issues and Impacts*, ASA Special Publication 65, Wisconsin, USA, 2003.
10. Giglio, L., Descloitres, J., Justice, C. O. and Kaufman, Y. J., An enhanced contextual fire detection algorithm for MODIS. *Remote Sensing Environ.*, 2003, **87**, 273–282.
11. Kaufman, Y. J. *et al.*, Potential global fire monitoring from EOS-MODIS. *J. Geophys. Res.*, 1998, **103**, 32215–32238.
12. Quinhan, J. R., *See5 Manual*, 2006; http://www.rulequest.com/see5-info.html

ACKNOWLEDGEMENTS. We thank Dr V. K. Dadhwal, Dean, Indian Institute of Remote Sensing, Dehradun for constant encouragement and useful suggestions during the course of their study.

Received 24 May 2007; revised accepted 14 March 2008